VIIRS Reflective Solar Bands On-Orbit Calibration Using the Moon

Junqiang Sun[1,2] and Menghua Wang[1]

[1]NOAA/NESDIS Center for Satellite Applications and Research,
5830 University Research Ct., College Park, MD 20740, USA
[2]Global Science and Technology, Inc., 7855 Walker Drive, Suite 200, Greenbelt, MD 20770, USA

ABSTRACT

The Visible Infrared Imager Radiometer Suite (VIIRS) has been on-orbit for more than three and half years. It has been scheduled to view the moon approximately monthly since its nadir door open on November 21, 2011. The scheduled lunar observations have been used to monitor the VIIRS reflective solar bands (RSB) on-orbit gain changes. The VIIRS RSB are primarily calibrated by an onboard Solar Diffuser (SD) panel and an accompanying Solar Diffuser Stability Monitor (SDSM). Due to non-uniformity of the SD degradation, the SD/SDSM calibration may have non-negligible errors, especially for the short wavelength bands. Since lunar surface is very stable, the Moon can be used to provide more reliable on-orbit long-term gain changes of the RSB. The RSB calibration coefficients derived from the lunar calibration are generally consistent with those derived from the SD/SDSM calibration, but clear differences in trend are seen, especially for the short wavelength bands.

***Index Terms*—** VIIRS, RSB, SD, SDSM, Calibration

1. INTRODUCTION

The Visible Infrared Imaging Radiometer Suite (VIIRS) on-board the Suomi National Polar-orbiting Partnership (SNPP) satellite was successfully launched on October 28, 2011 [1, 2]. It covers almost the entire Earth surface every day and collects visible and infrared imagery and radiometric measurements of the land, atmosphere, cryosphere and oceans. VIIRS has 22 spectral bands, among which 14 are reflective solar bands (RSB) covering a spectral range from 0.410 to 2.25 μm. The VIIRS RSB are calibrated on orbit with an on-board Solar Diffuser (SD) [3-5] with its degradation tracked by a Solar Diffuser Stability Monitor (SDSM) [6-8]. The VIIRS RSB on-orbit changes are also monitored with scheduled monthly lunar observations through the instrument's Space View (SV) [9, 10]. For VIIRS, the Angle of Incidence (AOI) of the SV is exactly the same as that of the SD. Thus, the lunar observation tracks the VIIRS RSB gain change at the same AOI as for the SD calibration. In principle, the two should provide the same on-orbit gain variation for all VIIRS RSB.

Figure 1. A lunar image.

In this study, we focus on the VIIRS RSB calibration using the Moon. Figure 1 is a lunar image, from which it is seen that the lunar surface is not smooth. Then lunar radiance cannot be directly used to derive the RSB calibration coefficients, called F-factors. Nevertheless, the lunar irradiance can be used to calibrate the RSB. The lunar irradiance varies with view geometry, and the lunar observations need to be carefully selected such that the view geometries to be as similar as possible in order to reduce the uncertainty of the lunar view geometric effect [11]. To increase lunar observation opportunity and possibility to select similar view geometries, an instrument roll maneuver is usually implemented for a scheduled lunar observation. The lunar view geometric effect on the lunar irradiance needs to be corrected if the lunar irradiance is used as reference to derive the RSB F-factors. The robotic lunar observatory (ROLO) model can provide the predicted lunar irradiance for various lunar view geometries [12]. The accuracy of the lunar calibration depends on that of the correction of the lunar view geometric effect. Any errors in the predicted lunar irradiance induce seasonal oscillations in the derived F-factors [5, 10, and 13]. It has been found that there are seasonal oscillations in the derived F-factors from the lunar observations due to the uncertainty of the ROLO model. In this analysis, a correction to the ROLO prediction is applied to reduce the oscillation.

We have analyzed and processed all the data of the lunar observations and calculated the RSB F-factors for the entire VIIRS mission. To distinguish the F-factors derived from the lunar calibration and from those derived from the

SD/SDSM calibration, the former are called lunar F-factors while the later called SD F-factors in this paper. In general, the derived lunar F-factors are consistent with those derived from the SD/SDSM observations. However, there are observable differences between the lunar and the SD F-factors, especially for the short wavelength bands [5, 10, 13]. It has been found that the SD degrades non-uniformly with respect to the incident and outgoing angles, resulting in errors in SD F-factors, especially in the short wavelength bands [8]. The differences confirm the non-negligible errors of the SD/SDSM calibration in the short wavelength range due to the non-uniformity of the SD degradation and also show the necessity of the lunar calibration for the VIIRS RSB. By combining the SD and lunar F-factors, a set of hybrid F-factors was developed and it was demonstrated that the hybrid F-factors significantly improved the accuracy and quality of VIIRS ocean color Environment Data Records (EDR) [14, 15].

In this paper, we review the lunar calibration algorithms and show some lunar calibration results. We also compare the lunar F-factors with the SD F-factors and discuss the advantages and disadvantages of the SD/SDSM and lunar calibrations. In Section 2, the lunar calibration algorithm is reviewed. In Section 3 the lunar observations are reviewed and data features are discussed. In Section 4, the F-factors derived from the lunar calibration are shown and compared with those derived from the SD calibration. The lunar calibration provides similar on-orbit gain changes for SNPP VIIRS RSB. But there are observable differences between the F-factors derived from the SD and lunar calibration for the short wavelength bands as previously mentioned. Section 5 summarizes and concludes the work.

2. LUNAR CALIBRATION ALGORITHMS

VIIRS views the Moon from its SV with the same AOI as the SD although their optical paths on the HAM are the reverse of each other. Being a well-studied target with a very stable reflectance in the visible and NIR spectral regions, the Moon can be used to track the VIIRS RSB gain change at the SD AOI. With the approximation that the detector difference is negligible, the detector averaged calibration coefficients, called lunar F-factors as mentioned earlier, can be expressed as [9]

$$f(B,M) = \frac{g(B)N_{t,M}}{\sum_{D,S,N} L_{pl}(B,D,S,N)\delta(M,M_N)}, \qquad (1)$$

where $g(B)$ corrects the relative geometric effects for band B, $N_{t,M}$ is the number of scans in the summation with HAM side M, N is scan number, S is pixel number along the scan direction, $L_{pl}(B,D,S,N)$ is the lunar irradiance calculated using the prelaunch calibration coefficients, and M_N is the side number of the scan N. In this analysis, we use the four scans mirror around the center of the lunar observation,

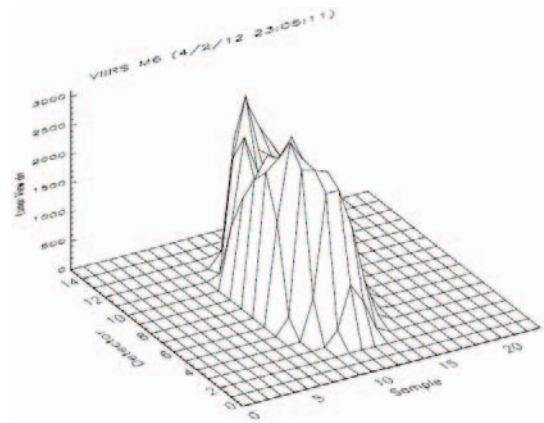

Figure 2. Lunar image observed by the band M6 on April, 2012.

during which the instrument scans the center of the lunar surface, to calculate the relative F-factor for each lunar calibration, two for each mirror side.

The lunar view geometry is described by Sun-Earth distance, sensor-moon distance, lunar phase angle, and lunar librations. The ROLO model can provide the predicted lunar irradiance for various lunar view geometries [12]. In other words, the lunar irradiance predicted by the ROLO model can be used as $g(B)$ to account for the geometric effect in Eq. (1). The absolute uncertainty of the ROLO model can be as large as ~5% for the short-wavelength bands and the uncertainty is even larger for the NIR bands [9]. However, the relative uncertainty of the irradiance predicted by the ROLO model over the entire view geometry is about 1% [12]. Since the lunar phase angle is confined to a selected region, the relative uncertainty of the lunar irradiance predicted by the ROLO model for VIIRS scheduled lunar observations should be smaller than 1%. Thus, the lunar calibration may not provide accurate absolute F-factors for VIIRS RSB, but it can provide relative F-factors or the on-orbit gain change since the first lunar observation. Since the relatively uncertainty of the ROLO model can be as large as ~1%, seasonal oscillations with amplitudes of ~0.5% are observed in the derived lunar F-factors. In this analysis, we introduce an extra correction for the lunar view geometry effect on top of the ROLO model for each RSB band to remove the seasonal oscillation. The correction is a function of libration angles.

Since the AOI for the SD and the SV is the same, the lunar and the SD/SDSM calibration track the on-orbit gain change at the same AOI and, then, should provide the same calibration coefficients or gain changes when they are normalized at any given time as mentioned previously.

3. LUNAR OBSERVATIONS AND DATA ANALYSIS

VIIRS views the Moon through its SV port. The size of the SV sector is about 0.85°. Therefore the view through the SV port forms a cone with a vertex angle of 0.85°. As VIIRS circles in its orbit, the Moon is viewed whenever it passes

into this cone view. A roll maneuver is a spacecraft rotation around the X-axis, the track direction. With a roll maneuver, the angular vertex ring formed by the view cone of the SV can change its size. With or without roll maneuvers, VIIRS can view the Moon for about nine months every year, which is different from the Moderate Resolution Imaging Spectroradiometer (MODIS). However, the roll maneuver does increase the opportunity to view the moon with about same phase angle, which is significantly important to reduce the uncertainty of the lunar F-factors derived from the lunar observations due to strong dependency of the lunar irradiance on the phase angle. To minimize the errors due to geometric effects, lunar views used for lunar calibration are selected such that the lunar phase angle is kept within a limited range. We originally chose [-55.5^o, -54.5^o] for VIIRS as the acceptable phase angle range, where the phase angle is defined to be negative for a waxing Moon and positive for a waning Moon. Later, the range was changed to [-51.5^o, -50.5^o] to minimize the roll angles required for the scheduled lunar observations which will be discussed in more detail later.

The Moon angular size is about 0.5^o, which corresponds to about 26 samples for M bands and 52 samples for I bands without aggregation. Since a sector rotation is applied to collect the data during a lunar observation, the lunar observation data are stored in the EV sector. An aggregation scheme is applied to VIIRS EV data. At the center of the EV, three detector footprints are aggregated to form a single VIIRS pixel. The scheme is applied to all VIIRS I bands and single-gain M bands. For dual-gain M bands, the scheme is applied to calibration data, but not the pre-calibrated instrument response. For lunar calibration, we only need the instrument response during a lunar observation. Thus, the sector rotation does not change the resolution of the dual-gain M bands, but it does reduce the resolution of the other bands. For a single-gain M band, the lunar size is about 8 aggregated pixels. Figure 2 displays the lunar image observed by band M6 in April 2012. It can be seen that lunar size along the scan direction is about 8 pixels as expected. To minimize the noise and meanwhile to have enough margins to fully cover the moon, we select 16 aggregated pixels centered at the center of the lunar image along the scan direction for a single gain M band in Eq. (1). For other bands, the number of pixel selected accordingly to ensure that they cover the same range that a single M band covers. The background response of the instrument for each band during a lunar observation is obtained from the pixels beyond the selected range.

4. LUNAR F-FACTORS

The gains, proportionally inverse to the F-factors, derived for SNPP VIIRS visible bands from the scheduled lunar observations are shown in Fig. 3 in symbols. Every year there are about three months in summer during which the

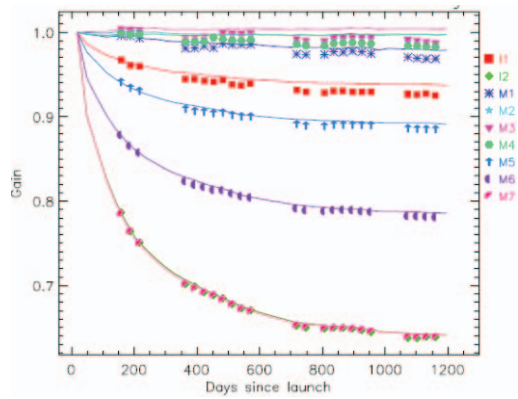

Figure 3. SNPP VIIRS visible and near infrared bands gains.

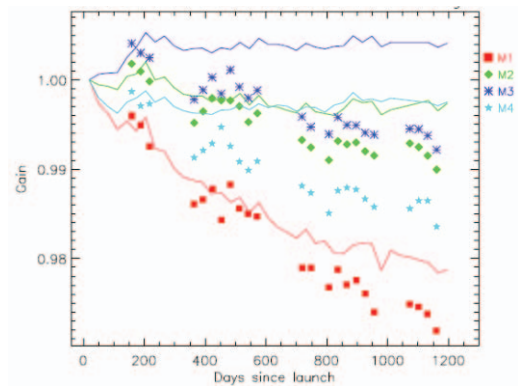

Figure 4. SNPP VIIRS visible bands F-factors.

SNPP VIIRS cannot see the moon even with roll maneuvers. These are reflected as data gaps in Fig. 3. For comparison, the corresponding gains derived from the SD/SDSM calibration are also drawn in the plots as lines. The gains are normalized at the time of the first scheduled lunar observation for each band. From the plot, it can be seen that the gains from the two calibrations agree with each other reasonably well for most bands but with differences between the two sets of gains, especially for the short wavelength bands. To clearly see the differences, Fig. 4 shows the gains derived from the SD/SDSM calibration and the lunar calibration only for bands M1-M4 with a smaller scale. No seasonal oscillations are observed in the lunar F-factors in Fig. 4 while they were seen in Fig. 3, where only ROLO model results are used to remove the geometric effect, and previous reports. As mentioned earlier, an extra correction on top of the ROLO model for the view geometric effect for each RSB, which removes the seasonal oscillation in the band's lunar F-factors or the gain trending. It is seen in Fig. 4 that there are obvious differences between the gains derived from the SD/SDSM calibration and those from the lunar calibration. It is also seen that the differences increase with time and the largest difference occurs in band M4, which is about 1.5%. The root cause of the differences between the two sets of gains for SNPP VIIRS short wavelength bands is partially due to the non-uniformity of SD degradation with respect to incident solar angles and

view angles, which results in SD degradation differences for the SDSM view direction and that of the RSB. This difference induces SD calibration errors, especially in the short wavelength bands.

The non-uniformity of the SD degradation implies a serious deficiency in the current SD/SDSM calibration methodology. Compared to SD/SDSM calibration, the lunar calibration based on irradiance, however, faces no such degradation issue [16] and then in principle should provide more reliable and accurate long-term RSB gain on-orbit change, especially for the short wavelength bands. Thus, the lunar calibration can provide a successful mitigation approach, to be referred to as "hybrid", based on both SD and lunar calibrations to derive the correct F-factors. This mitigation method has already been completed and some preliminary results have already been reported in several public forums. It was demonstrated that the new lookup tables (LUTs) generated with the "hybrid" F-factors remove the long-term drifts in EDR ocean color products, compared with results from the LUTs generated only using the SD F-factors. The new F-factors from the hybrid method significantly improve the quality of the ocean color EDR. Details of the "hybrid" approach and the evaluation of the improvements of new hybrid F-factors on the ocean color products will be discussed elsewhere.

5. SUNMARY

We have presented the on-orbit VIIRS RSB calibration using the Moon for VIIRS and the updated three-and-half-year lunar calibration coefficients for the RSB. The calibration coefficients are smooth and stable. They are strongly band dependent as expected. The lunar calibration coefficients are compared with those from the SD/SDSM calibration. They generally agree with each other, but some obvious differences are observed, especially for the VIIRS short wavelength bands. The differences can be as large as ~1.5% and they are partially induced by the non-uniformity of the SD degradation with respect to incident and outgoing angles. Compared to the SD/SDSM calibration, the lunar calibration can provide more reliable long-term on-orbit gain changes for the VIIRS short wavelength bands and provide a mitigation approach to overcome the deficiency of the SD/SDSM calibration method.

ACKNOWLEDGMENTS

This work was supported by JPSS/VIIRS funding. We would like to thank Xiaoxiong Xiong, Vincent Chiang, and Jon Fulbright and other VCST members for providing us verified Raw Data Records (RDR) data for the lunar observations used in this analysis and other related information. The views, opinions, and findings contained in this paper are those of the authors and should not be construed as an official NOAA or U.S. Government position, policy, or decision.

REFERENCES

[1] C. Cao, et al, "Early on-orbit performance of the Visible Infrared Imaging Radiometer Suite (VIIRS) onboard the Suomi National Polar-orbiting Partnership (S-NPP) satellite," *IEEE Trans. Geosci. Remote Sens.*, 52, 1142–1156 (2014).

[2] Xiong, et al, "VIIRS on-orbit calibration methodology and performance," *J. Geophys. Res. Atmos*., 119, 5065–5078 (2014).

[3] N. Lei, et al, "Initial on-orbit radiometric calibration of the Suomi NPP VIIRS reflective solar bands," *Proc. SPIE*, 8510, 851018 (2012).

[4] C. Cardema, et al, "Operational calibration of VIIRS reflective solar band sensor data records," *Proc. SPIE*, 8510, 851019 (2012).

[5] J. Sun and M. Wang, "VIIRS Reflective Solar Bands On-Orbit Calibration and Performance: A Three-Year Update," *Proc. SPIE*, 9264, 92640L (2014).

[6] J. Fulbright, et al, "Characterization and performance of the Suomi-NPP VIIRS solar diffuser stability monitor," *Proc. SPIE*, 8510, 851015 (2014).

[7] E. Hass, et al, "VIIRS solar diffuser bidirectional reflectance distribution function (BRDF) degradation factor operational trending and update," *Proc. SPIE*, 8510, 851016 (2012).

[8] J. Sun and M. Wang, "Visible Infrared Imaging Radiometer Suite solar diffuser calibration and its challenges using a solar diffuser stability monitor," *Appl. Opt*., 53, 8571-8584 (2014).

[9] J. Sun, X. Xiong, and J. Butler, "NPP VIIRS on-orbit calibration and characterization using the moon," *Proc. SPIE*, 8510, 85101I (2012).

[10] X. Xiong, J. Sun, J. Fulbright, and Z. Wang, "Lunar Calibration and Performance for S-NPP VIIRS Reflective Solar Bands," submitted to *IEEE Trans. Geosci. Remote Sens.*.

[11] J. Sun and X. Xiong, "Solar and lunar observation planning for Earth-observing sensor", *Proc. SPIE*, **8176**, 817610, (2011).

[12] H. H. Kieffer and T. C. Stone, "The spectral irradiance of the Moon," *Astron. J.*, 129, 2887–2901 (2005).

[13] E. Eplee Jr., et al, "On-orbit calibration of the Suomi National Polar-orbiting Partnership Visible Infrared Imaging Radiometer Suite for ocean color applications," *Appl. Opt.*, 54, 1984–2006 (2015).

[14] M. Wang, et al, "Evaluation of VIIRS ocean color products," *Proc. SPIE,* 9261, 92610E (2014).

[15] M. Wang, "Remote sensing of the ocean contributions from ultraviolet to near-infrared using the shortwave infrared bands: simulations," Appl. Opt., 46, 1535–1547 (2007).

[16] H. H. Kieffer, "Photometric stability of the lunar surface," *Icarus*, 130, 323–327 (1997).